Measuring High-Slope and Super-Smooth Optics with High-Dynamic-Range Coherence Scanning Interferometry

Martin F. Fay, Xavier Colonna de Lega, and Peter de Groot
Zygo Corporation, Laurel Brook Lane, Middlefield, Connecticut, USA 06455
mfay@zygo.com

Abstract: Advances in the implementation of coherence scanning interferometry have dramatically extended the range of application for this well-known technique. New data acquisition and data processing methods significantly improve dynamic range, enabling measurements of steeply-sloped surfaces usually considered beyond the reach of high-NA objectives. Hybrid data acquisition incorporating sinusoidally-modulated phase shifting reduces signal-to-noise to the 0.1 nm/√Hz level, extending the technique to super-polished surfaces.
OCIS codes: 120.3180 Interferometry; 120.3940 Metrology; 120.6660; Surface measurements, roughness

1. Introduction

Optical components present a number of metrology challenges, including reflectances ranging from mirror-like to anti-reflective, slopes from normal to near-vertical, and surface roughness from multi-µm to sub-Å. For optical metrology, these collectively correspond to signal strengths spanning several orders of magnitude.

Coherence scanning interferometry (CSI) provides non-contact areal topography maps with typical single-measurement topography repeatability on smooth, high-reflectivity surfaces of less than a nm [1, 2]. Recent advances in the technology both significantly improve the baseline sensitivity of CSI and enable high-dynamic-range operation. High-dynamic-range CSI can measure previously-inaccessible high slopes and sub-Å roughness, capabilities well-suited for measuring optical components.

2. Measurement and analysis

A modern commercial CSI microscope was used to measure a variety of challenging optical components [3]. The following sections each highlight a different technique to boost dynamic range: dynamic noise reduction (DNR) for detection of weak signals; high dynamic range (HDR) for parts with wide reflectance ranges; and CSI combined with sinusoidally-modulated phase shifting interferometry (PSI) for measurement of low-departure super-smooth surfaces. For these experiments, the CSI data acquisition rate is 0.14 seconds per micron scanned. All surface plots shown represent raw height data without smoothing, masking or interpolation of missing data points.

3. Dynamic noise reduction (DNR)

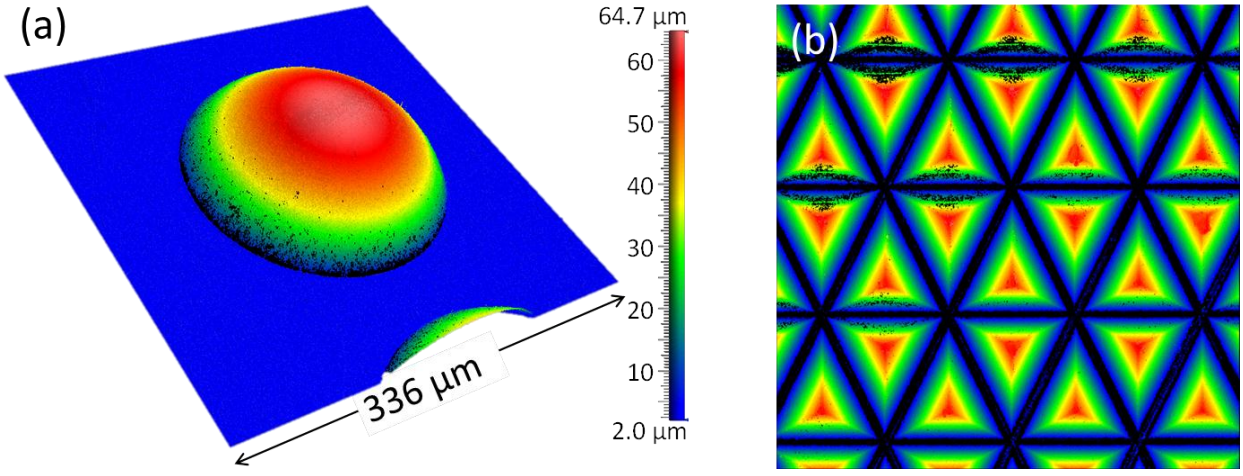

Fig. 1. Measurements of (a) polymer micro-lens using 3X DNR; and (b) retroreflector array using 4X DNR.

For an ideal measurement setup the highest observed slope θ_{max} is accommodated within the specular limit of the objective NA, satisfying $NA > \sin(\theta_{max})$. However, in practice a lower-NA objective may be prescribed by

technical bounds on minimum working distance or field-size/throughput; or by practical considerations such as cost and availability. Fortunately, measuring slopes beyond the specular limit is possible provided some light is scattered *and* the measurement is sufficiently sensitive. If the latter condition is not satisfied, DNR allows a user-specified trade-off between throughput and sensitivity with no other performance sacrifice.

Fig. 1(a) shows an example of a polymer microlens measured with a 50X Mirau objective with NA = 0.55 and a corresponding specular limit of $\sin(\mathrm{NA}) \cong 33°$. A conventional CSI measurement might yield only sparse data for the higher slopes, but also a valuable hint: data at slopes above the specular limit suggest detectable scattered light. With 3X DNR (9X increase in measurement time), data coverage is near-complete with measured slopes up to 60°.

Fig. 1(b) shows a retroflector array formed in uncoated mirror-finish polymer, with slopes beyond the specular limit and the additional confound of a strong retro-reflection decoy signal. Again, conventional CSI yields only sparse data but also an indication of scattered light given discerned slopes of ~60° (north-south) and of ~52° (diagonal). With 4X DNR (16X increase in measurement time), data coverage is complete on the diagonal sides, and considerably improved for the higher-slope north-south sides. Drop-out in the grooves is due to near-overlap of the desired surface signal with the strong retroreflection signal, and represents opportunity for further improvement.

DNR is also applicable for low-magnification measurements, such as measuring the form of ground glass.

4. High dynamic range (HDR)

Dynamic range can be extended more efficiently for parts having a wide range of reflectance. For a traditional CSI measurement, light level is chosen so as to avoid sensor saturation and hence is driven by the highest reflectance in the scene. This doubly penalizes low-reflectance regions, already more prone to data drop-out due to their low-contrast interferometric signal, by additionally light-starving them.

Schmit *et al* propose two approaches [4]. The first is restricted to parts comprising known disparate reflectances at known well-separated scan locations: light level is changed between optimized values midway between the reflectance populations. A second approach is generally applicable, including for parts having reflectance populations intermixed along the scan dimension: scanning is performed at half speed, with light level switching between two prescribed values at each camera frame. Thus two interleaved scans are performed simultaneously, with results combined afterwards. This approach requires *a priori* selection of light levels.

The HDR approach presented here begins by scanning at a standard non-saturating light level, dictated by the highest-reflectance region in the scene. Results are then analyzed to optimize higher light level(s) for follow-on scan(s) catering to lower-reflectance features. The final height map combines the best results all constituent scans. The process is fully automated and generally applicable, requiring no prior knowledge of reflectance extrema or their relative scan location.

For an extreme demonstration, Fig. 3 shows a test sample comprising adjacent regions of chrome and an anti-reflection (AR) coating, with approximate reflectances of 90% and 0.3% respectively, for a dynamic range of 300:1. This sample was measured using a 5X Michelson (NA = 0.13). The first HDR scan favors the chrome, yet manages to get data everywhere in the AR region in spite of its intensity being barely discernible from the intervening gap. This facilitates incorporating results from a second scan performed at an automatically determined light level favoring the AR surface, revealing its detailed features and local S_a of about 2 to 3 nm. Without the second HDR scan the measured S_a is ~10 nm, driven by measurement noise. Total measurement time is only twice that of a conventional CSI scan, compared to 16X for comparable DNR results.

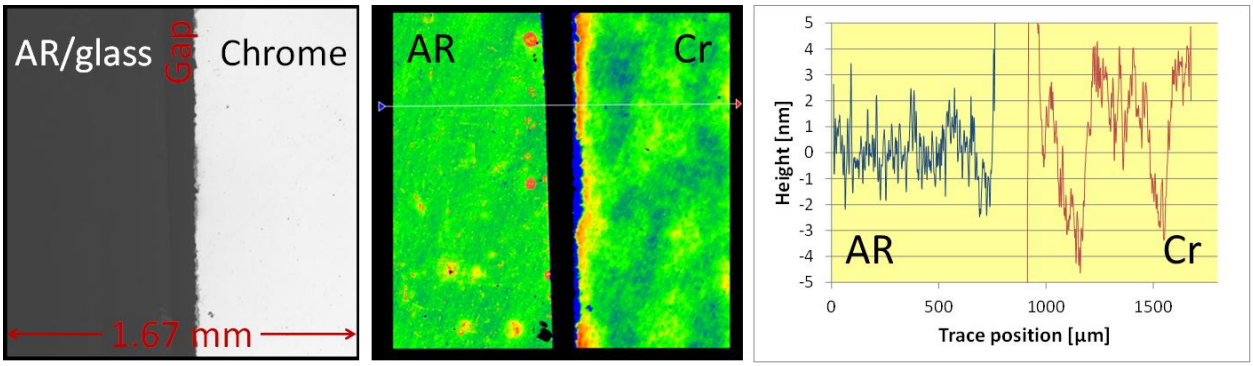

Fig. 2. Measurement of adjacent AR and chrome. *Left:* intensity image at non-saturating light level; *middle:* height map from HDR measurement; *right:* horizontal trace through AR and chrome.

5. Noise reduction using CSI combined with PSI

Many optical components have low departure and surface roughness below the noise floor of conventional CSI. Phase-shifting interferometry (PSI) is often used to measure such parts, with successive phase-shift cycles efficiently reducing measurement noise [5, 6]. However, finding focus can be challenging, and PSI cannot resolve relative fringe order for discontinuous features such as steps.

A known solution is to combine the strengths of CSI and PSI [7]. An initial coherence scan autofocuses the part and determines relative fringe order over then scene. A subsequent PSI measurement improves the noise level. Modern versions of this concept include several improvements, including the use of Fourier methods to determine the equivalent wavelength for the PSI measurement, and sinusoidal PSI modulation to enable continuous, high-speed data acquisition over a number of cycles N chosen according to the desired noise level [8, 9]. This sequence also includes an in-situ wavelength calibration that empirically incorporates scanner motion, obliquity, source uniformity, and part-dependency. PSI offers the fastest $\sqrt{N}$ scaling for a given target noise level, with an effective noise bandwidth of about 0.1 $\mathrm{nm}/\sqrt{\mathrm{Hz}}$ [3].

Example results are shown in Fig. 4. With 16 cycles (3 sec), grain boundaries on a SiC flat can be discerned. A 256-cycle (52 sec) measurement reports a local S_a of about 22 pm for a super-smooth optic. Finally, a measurement of a 1.8-µm step-height standard demonstrates accommodation of multi-fringe-order discontinuities.

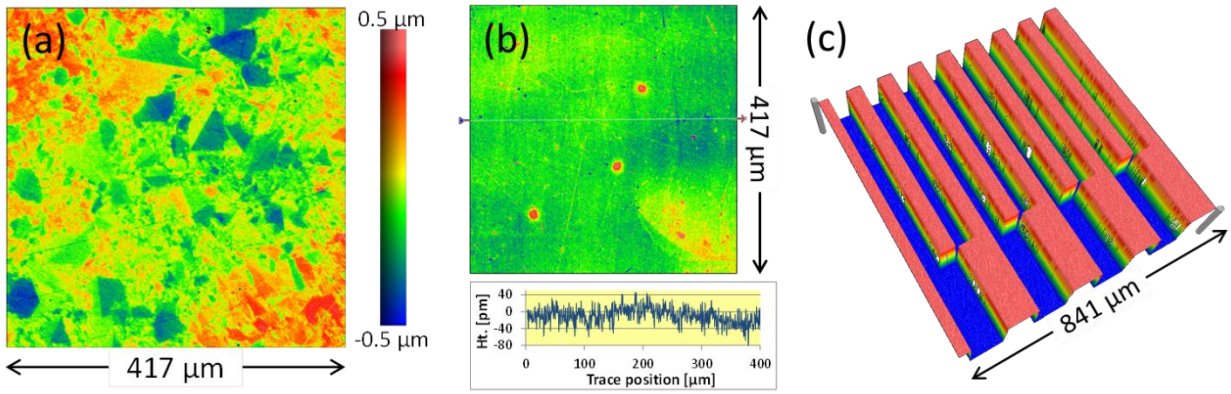

Fig. 3. Hybrid CSI/PSI results: (a) grains of SiC 'flat' measured using a 20X Mirau (NA = 0.4); (b) roughness of super-smooth optic, also measured with 20X Mirau; and (c) discontinuous 1.8-µm steps measured using a 5X Michelson (NA = 0.13).

6. Conclusion

Recent advances dramatically extend the applications reach of CSI for measuring challenging optical components, with both improved baseline sensitivity and more tools to further extending dynamic range. Previously inaccessible slopes and scattering surfaces can now be measured, and sub-Å measurements efficiently performed.

References

[1] de Groot, P. "Coherence Scanning Interferometry," [Optical Measurement of Surface Topography], R. Leach, Ed., Springer Verlag, Berlin, 9 (2011).
[2] ISO, [25178-604:2013(E): Geometrical product specification (GPS) – Surface texture: Areal – Nominal characteristics of non-contact (coherence scanning interferometric microscopy) instruments] International Organization for Standardization, Geneva (2013).
[3] Zygo Corporation, [NexView Optical Profiler], Specification sheet SS-0095 09/12 (2013).
[4] Schmit, J., and Harasaki, A., "High-precision interferometric shape measurement of objects with areas of different reflectance," Proc. SPIE 4275, 85-93 (2001).
[5] Schreiber, H., and Bruning, J. H. "Phase Shifting Interferometry," [Optical Shop Testing], D. Malacara, Ed., John Wiley & Sons, Inc., (2006).
[6] de Groot, P. "Phase Shifting Interferometry," [Optical Measurement of Surface Topography], R. Leach, Ed., Springer Verlag, Berlin, 8 (2011).
[7] Ai, C., and Caber, P. J., "Combination of white-light scanning and phase-shifting interferometry for surface profile meaurements," US Patent 5,471,303 (1995).
[8] de Groot, P., "Design of error-compensating algorithms for sinusoidal phase shifting interferometry," Applied Optics 48(35), 6788 (2009).
[9] de Groot, P., "Sinusoidal Phase Shifting Interferometry," US Patent 7,933,025 (2011).